2.     H-atom concentrations generally satisfy the requirements of local thermodynamic equilibrium within the soot growth region of laminar premixed flames (which is well downstream of the main reaction zone). This observation is justified by both measurements and predictions of flame structure and is perhaps not surprising due to the relatively slow evolution of the properties of the soot growth region.

3.     Even though yields of H concentrations approximate local thermodynamic equilibrium, the yields of major gas species clearly are not in local thermodynamic equilibrium, e.g., the concentrations of these species typically depart from equilibrium requirements by factors greater than 3.

Corresponding major conclusions drawn from the observations of the diffusion flames are as follows:

1.     Measurements show that H, OH and O approach equilibrium near the start of the soot formation region but generally exhibit superequilibrium concentrations (by factors in excess of 10-20) throughout the soot formation region.

2.     Measurements show that soot formation in the diffusion flames studied during this investigation generally involves the decomposition of the original fuel to form relatively robust substances such as $C_2H_2$, $CH_4$, $H_2$ and the radicals H, OH and O. Subsequently, soot formation mainly involves the reaction of acetylene and H through the HACA mechanism (which will be demonstrated subsequently). This behavior was observed even when an aromatic compound, e.g., benzene that might be thought to emphasize soot formation paths involving PAH, was present.

3.     Measurements showed that significant degrees of net soot formation begins when H first appears and ends when acetylene concentrations become small, highlighting the importance of H and acetylene for the formation of soot in diffusion flames.

③ / cw / IN / 25         2001168955      547600

## 3. Soot Reaction Properties (Ground-Based Study)

Ins 15

### 3.1 Introduction

Three major soot reaction processes are needed to predict soot properties in flame environments: soot growth, or the formation of soot on soot nuclei and soot particles; soot oxidation, or the reaction of soot with oxidizing species to yield the combustion products of soot

oxidation; and soot nucleation, or the formation of soot nuclei from soot precursors having large molecular weights (generally thought to be large and particularly stable PAH molecules in flame environments, called stabilomers). These processes are addressed in the following, considering soot growth, oxidation and nucleation, in turn, by exploiting the soot and flame structure results for premixed and diffusion flames already discussed in Section 2. The following discussion is brief, see Xu et al. (1997,1998,2000a,2000b), Xu and Faeth (2000,2001) and El-Leathy et al. (2001) for more details.

## 3.2 Soot Growth

**Soot Growth Rate Properties**. Present measurements were used to find soot growth and nucleation rates, similar to earlier studies in laminar diffusion flames, e.g., Sunderland et al. (1995), Sunderland and Faeth (1996) and Lin et al. (1996). Major assumptions were similar to this earlier work, as follows: soot surface growth rather than soot nucleation, dominates soot mass production; effects of diffusion (Brownian motion) and thermophoresis on soot motion are small, so that soot particles convect along the axis of the flames at the local gas velocity; the soot density is constant; and the surface area available for soot growth is equivalent to that of constant diameter spherical primary soot particles that meet at a point. The justification for these assumptions can be found in Xu and Faeth (2001) and references cited therein.

Given these assumptions, the soot properties needed to find soot nucleation and growth rates can be found from the measurements of Xu and Faeth (2001). The number of primary particles per unit volume, $n_p$, is found from measurements of soot volume fractions and primary soot particle diameters, as follows:

$$n_p = 6f_s/(\pi d_p^3) \tag{1}$$

The soot surface area per unit volume of the flow, S, is then found from the same measurements, as follows:

$$S = \pi d_p^2 n_p = 6f_s/d_p \tag{2}$$

Defining soot surface growth rate, $w_g$, as the rate of increase of soot mass per unit soot surface area and time, conservation of soot mass along a stream under the previous assumptions yields (Sunderland et al.,1995):

$$w_g = (\rho/S)d(\rho_s f_s/\rho)/dt \tag{3}$$

Finally, the soot nucleation rate, $w_n$, was defined as the rate of increase of the number of primary particles per unit volume and time. Then based on the previous assumptions, the expression for the soot nucleation rate becomes (Sunderland et al.,1995):

$$w_n = \rho d(n_p/\rho)/dt \tag{4}$$

The gas density needed in Eqs. (3) and (4) was found from present measurements of major gas species concentrations and temperatures, assuming an ideal gas mixture and neglecting the volume of soot (which was only present at ppm levels); the soot density needed in Eq. (3) was taken to be 1850 kg/m$^3$, as discussed by Sunderland et al.(1995), and the temporal derivatives needed in Eqs. (3) and (4) were found from three-point least-square fits of the arguments of the derivatives.

The gross soot growth rates obtained from Eq. (3) were corrected for soot oxidation in the same manner as Sunderland et al.(1995): soot oxidation by O and OH were ignored, soot oxidation by $O_2$ was based on the results of Nagle and Strickland-Constable (1962), and soot oxidation by $H_2O$ and $CO_2$ were estimated following Libby and Blake (1979,1981). These corrections were only applied where estimated soot oxidation rates never exceeded half the gross soot growth rates. Subsequently, soot oxidation in diffusion flames were resolved as discussed in the next section, finding that oxidation by OH was dominant, similar to the findings of Neoh et al. (1980) for premixed flames. The present concentration estimates of soot oxidation rates, however, had little effect on estimated soot growth rates so that the new estimates of soot oxidation rates caused negligible changes in the measured growth rates.

**Soot Growth Mechanisms.** Soot surface growth rates were interpreted by using the HACA mechanisms of Frenklach and Wang (1990,1994), Kazakov et al. (1995) and Colket and Hall (1994). The mechanism of Kazakov et al. (1995) can be summarized as follows:

$$C_s - H + H \rightarrow C_s^* + H_2 \tag{R1}$$

$$C_s^* + H_2 \rightarrow C_s - H + H \tag{-R1}$$

$$C_s^* + H \rightarrow C_s - H \tag{R2}$$

$$C_s^* + C_2H_2 \rightarrow C_s - H + H \tag{R3}$$

where $C_s - H$ represents an armchair site on the soot particle surface and $C_s^*$ represents a corresponding radical site. The resulting net rate of soot particle surface growth for this mechanism was expressed as:

$$w_g = \alpha_{FW} R_{FW} \qquad (5)$$

where the parameter $\alpha_{FW}$ is an empirical (steric) factor of order of magnitude unity which involves corrections where sites on carbonaceous surfaces are treated analogous to corresponding sites on gaseous PAH molecules, whereas, $R_{FW}$, represents the appropriate reaction rate resulting from the mechanism of Eqs. (R1)-(R3) as described by Kazakov et al. (1995), see Xu et al. (1997) for the specific form of $R_{FW}$ used during present work. Kazakov et al. (1995) suggest that $\alpha_{FW}$ should be a function of temperature; therefore, it was correlated in terms of an Arrhenius function of temperature during present work. Colket and Hall (1994) add additional steps to the mechanism of Eqs. (R1)-(R3) in an attempt to explain the temperature dependence of $\alpha_{FW}$. This yields an extended HACA mechanism which can be represented as

$$w_g = \alpha_{CH} R_{CH} \qquad (6)$$

where the specific expression for $R_{CH}$ can be found in Xu et al. (1997) and $\alpha_{CH}$ is an empirical constant steric factor having a value on the order of unity.

**Evaluation of Soot Growth Mechanisms.** For the conditions in the laminar premixed and diffusion flames considered during the present investigation, both $R_{FW}$ and $R_{CH}$ are proportional to the product $[H][C_2H_2]$ as a first approximation, thus $w_g/[C_2H_2]$ measured during all the soot growth studies undertaken during the report period, Xu et al. (1997,1998), Xu and Faeth (2001) and El-Leathy et al. (2001), are plotted as a function of $[H]$ in Fig. 9 in order to provide a direct test of the main features of the HACA soot growth mechanisms without the intrusion of uncertainties due to the numerous empirical parameters in the original detailed mechanisms of Frenklach and Wang (1990,1994), Kazakov et al. (1995) and Colket and Hall (1994). The results for premixed and diffusion flames are distinguished by denoting them with open and dark-bordered or closed symbols, respectively. The correlation of the results according to the approximate HACA mechanism is seen to be surprisingly good. There is no significant effect of fuel type within the groupings of measurements for premixed and diffusion flames. Even results for premixed and diffusion flames compare reasonably well, with only a slight tendency for diffusion flames to exhibit a somewhat larger soot growth rate for comparable values of $[H]$ and $[C_2H_2]$. This last effect may be due to the use of the thermodynamic equilibrium approximation for $[H]$ in the premixed flames whereas direct measurements of $[H]$
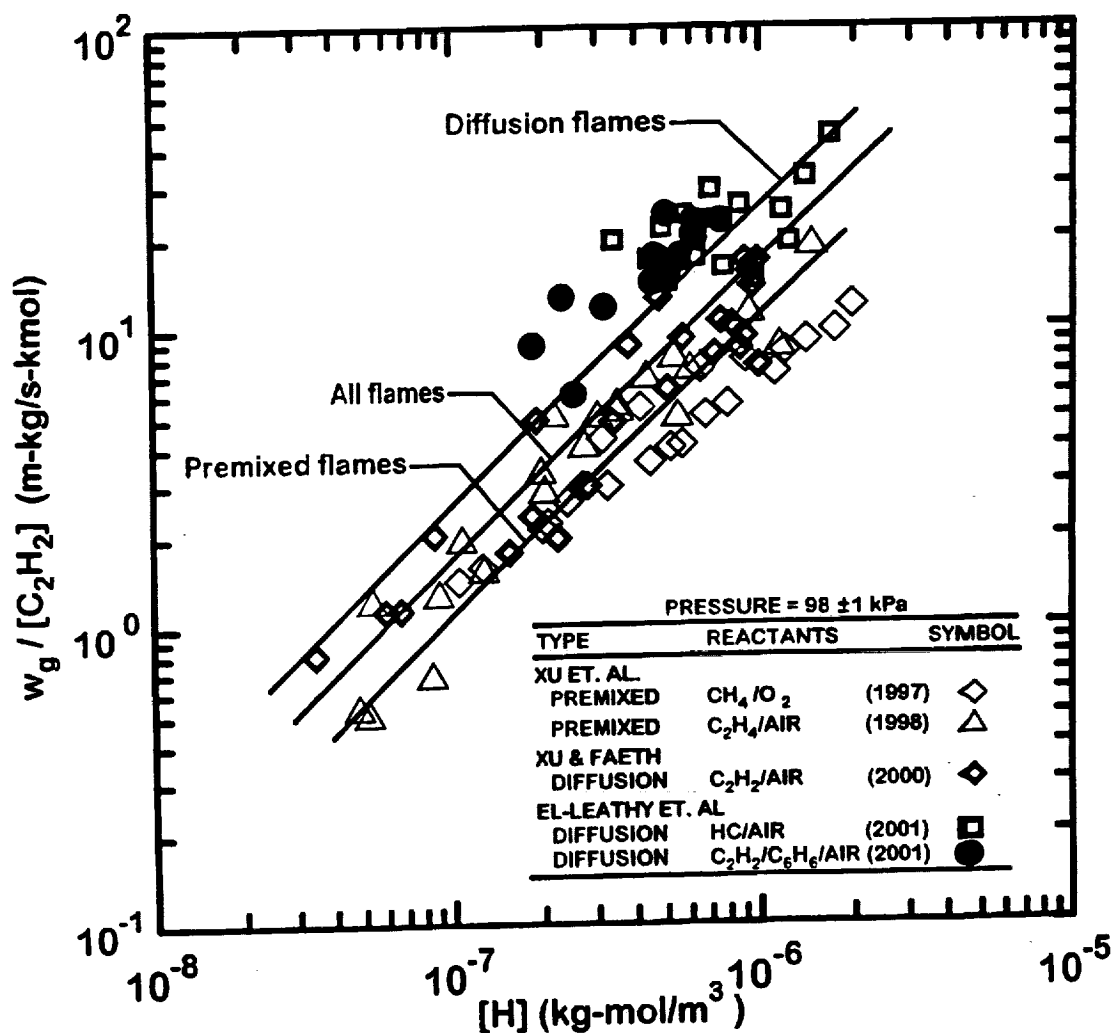
Fig. 9 Soot surface growth rates (corrected for soot oxidation) as a function of acetylene and hydrogen radical concentrations for laminar premixed and diffusion flames at atmospheric pressure. Measurements for ethylene/air premixed flames from Xu et al.(1997), measurements of methane/oxygen premixed flames from Xu et al. (1998), measurements of acetylene-nitrogen/air diffusion flames from Xu and Faeth (2001) and measurements of hydrocarbon-nitrogen/air diffusion flames from El-Leathy et al. (2001).

were used for the measurements of soot growth rates in diffusion flames. In particular, measurements in premixed flames generally showed that measured values of [H] were somewhat smaller than values estimated assuming chemical equilibrium, see Fig. 5. In any event, differences between estimates of soot growth rates for various fuel types and premixed and diffusion flame conditions generally approach anticipated differences due to experimental uncertainties and are supportive of the main features of the HACA mechanisms for soot growth.

More direct evaluations of the HACA mechanisms of soot surface growth can be obtained by plotting $w_g$ directly as a function of $R_{FW}$ or $R_{CH}$. The results for the mechanism of Colket and Hall (1994) are illustrated in Fig. 10. Correlations of all the flames and only the diffusion flames are seen to agree reasonably well with results for only the premixed flames suggesting somewhat smaller growth rates for premixed flames than diffusion flames at comparable conditions, as just discussed. The correlation for all the flames also yields a steric factor of 0.9 which is quite reasonable. Findings using the mechanism of Frenklach and Wang (1995) were similar. Thus present measurements of soot growth rates in laminar premixed and diffusion flames suggest small effects of fuel type in both premixed and diffusion flames and generally are supportive of the HACA mechanisms for soot growth.

## 3.3 Soot Oxidation

**Soot Oxidation Rate Properties**. Present measurements were used to find soot oxidation rates, using methods analogous to the soot growth rate measurements. After finding $n_p$ and S as described in connection with Eqs. (1) and (2), the expression for the soot oxidation rate per unit soot surface area, $w_{ox}$, becomes (El-Leathy et al., 2001):

$$w_{ox} = - (\rho/S)d(\rho_s f_s)/\rho)dt \qquad (7)$$

where the various terms in soot oxidation expression of Eq. (7) were found in the same manner as the soot growth and nucleation rate expressions of Eqs. (3) and (4). The minus sign is inserted so that $w_{ox}$ is a positive number.

The measurements of soot oxidation were corrected for effects of soot growth using the soot growth estimates of Colket and Hall (1994); no condition was considered, however, where the correction for soot growth was more than half the soot oxidation rate. Finally, in order to avoid problems of effects of particle surface porosity and internal particle oxidation observed by Neoh et al. (1984), present observations of soot surface oxidation rates were limited to conditions where less than 70% of the maximum soot mass had been oxidized.
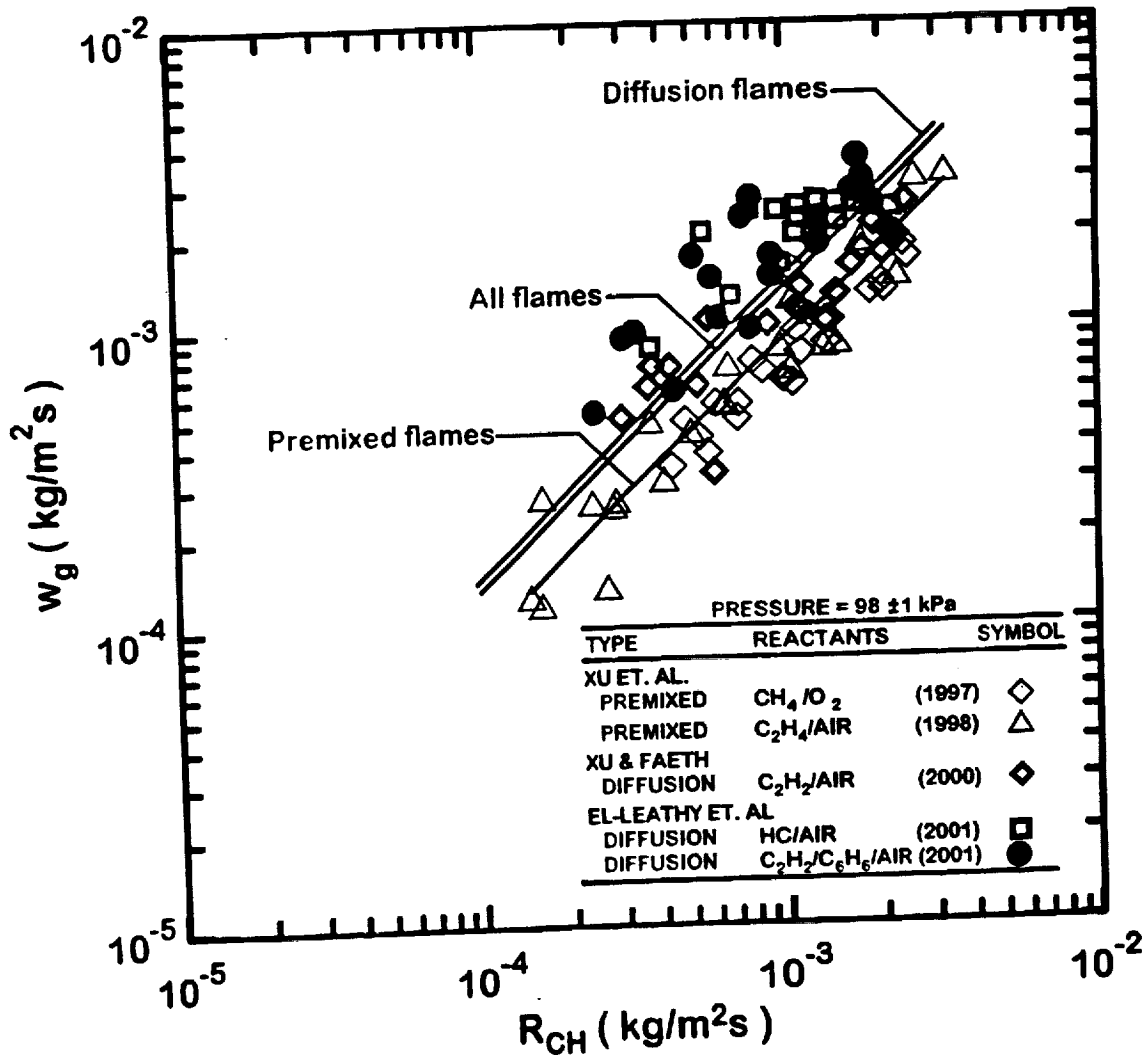
Fig. 10 Soot surface growth rates (corrected for soot oxidation) in terms of the HACA mechanism of Colket and Hall (1994) for laminar premixed and diffusion flames at atmospheric pressure. Measurements for ethylene/air premixed flames from Xu et al. (1997), measurements of methane/oxygen premixed flames from Xu et al. (1998), measurements of acetylene-nitrogen/air diffusion flames from Xu and Faeth (2001) and measurements of hydrocarbon-nitrogen/air diffusion flames from El-Leathy et al. (2001).

**Soot Oxidation Mechanisms.** Similar to Neoh et al. (1980), present soot oxidation rates (corrected for soot growth) were converted into collision efficiencies based on kinetic theory estimates of the collision rates of given gas species with the surfaces of primary soot particles. Thus, the collision efficiency, $\eta_i$, for a potential oxidizing species i, is given by the following expression (Sunderland and Faeth, 1996):

$$\eta_i = 4w_{ox}/(C_i[i]\,\bar{v}_i) \tag{8}$$

where $C_i$ is the mass of carbon removed from the surface per mole of species i reacting at the surface, [i] is the gas phase concentration of species i adjacent to the surface, and

$$\bar{v}_i = (8kT/(\pi M_i))^{1/2} \tag{9}$$

is the (Boltzmann) equilibrium mean molecular velocity of species i.

**Evaluation of Soot Oxidation Mechanisms.** Collision efficiencies of $O_2$ for soot oxidation are plotted as a function of height above the burner in Fig. 11. Results shown on the figure include the range of values observed by Neoh et al. (1980) in premixed flames, the values observed from the present experiments in diffusion flames, and values estimated from the predictions. Results shown on the figure include the range of values observed by Neoh et al. (1980) in premixed flames, the values observed from the present experiments in diffusion flames, and values estimated from the predictions of Nagle and Strickland-Constable (1962) for the conditions where present measurements were made in diffusion flames. The Nagle and Strickland-Constable (1962) approach has exhibited effective capabilities to predict soot oxidation by $O_2$ and there are significant levels of $O_2$ along the present soot paths, see Figs. 6 and 8. Thus, the fact that the Nagle and Strickland-Constable (1962) estimates of the $O_2$ collision efficiencies are 10-100 times smaller than the present measurements strongly suggests that some other species is mainly responsible for soot oxidation in the present flames. Other evidence that $O_2$ is not the main direct soot oxidizing species for flame environments is provided by the large scatter (nearly a factor of 100) of the present $O_2$ collision efficiencies for diffusion flames combined with even the larger scatter (more than a factor of 100) of the $O_2$ collision efficiencies of Neoh et al. (1980) in premixed flames.

The collision efficiencies of $CO_2$, $H_2O$ and O exhibited similar unsatisfactory correlations for early soot oxidation rates in premixed and nonpremixed flames (Neoh et al., 1980; Xu et al., 2000a). The collision efficiencies of OH for soot oxidation are plotted as a function of height above the burner in Fig. 12, in the same manner as the results for $O_2$ in Fig. 11. With perhaps one exception, at a marginal condition where rates of oxidation were small, direct $O_2$ oxidation
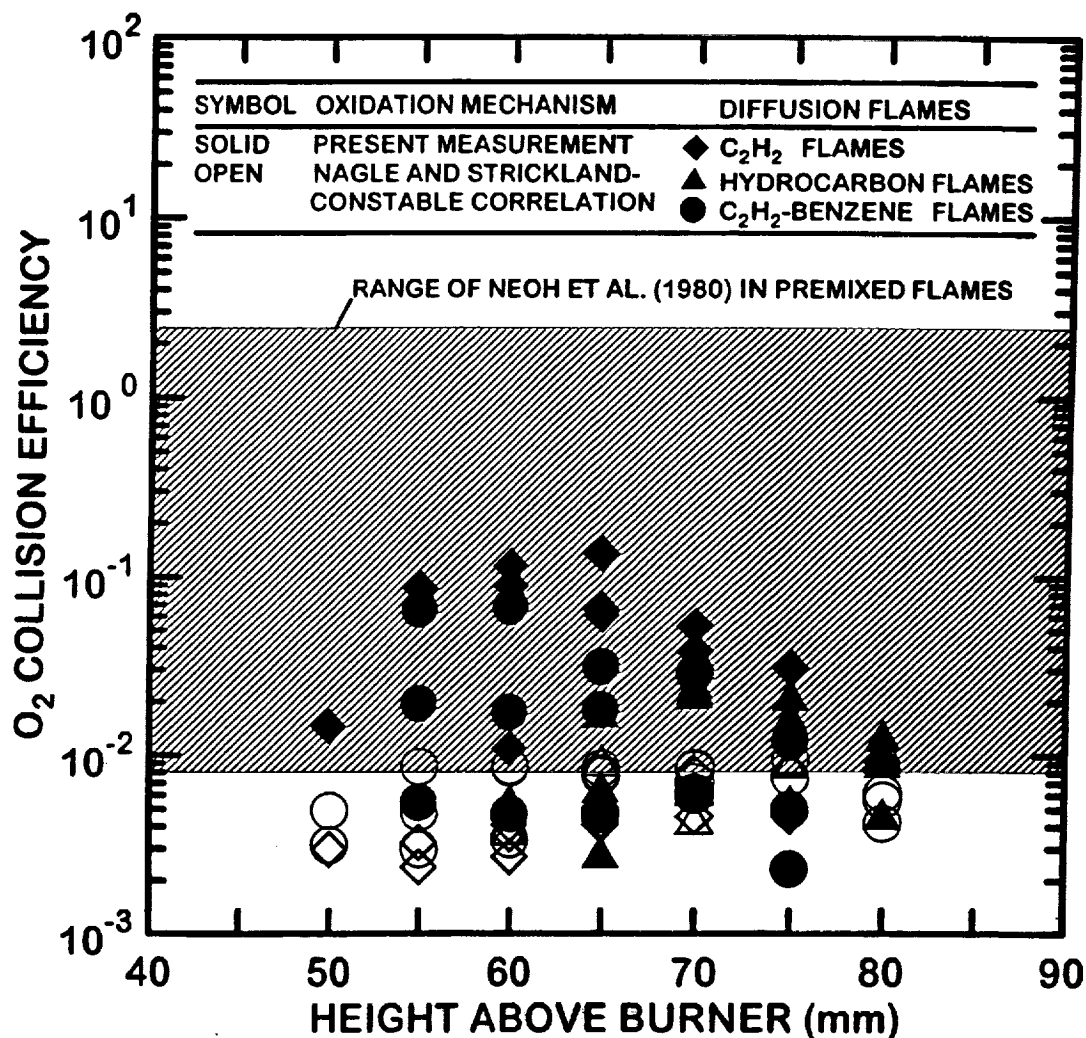
Fig. 11    Collision efficiencies assuming soot burnout due to attack by $O_2$ as a function of height above the burner at atmospheric pressure. Found from the measurements of Neoh et al. (1980) in premixed flames, estimated from the predictions of Nagle and Strickland-Constable (1962) for the conditions of the present diffusion flames and found from present measurements in diffusion flames. From Xu et al. (2001).
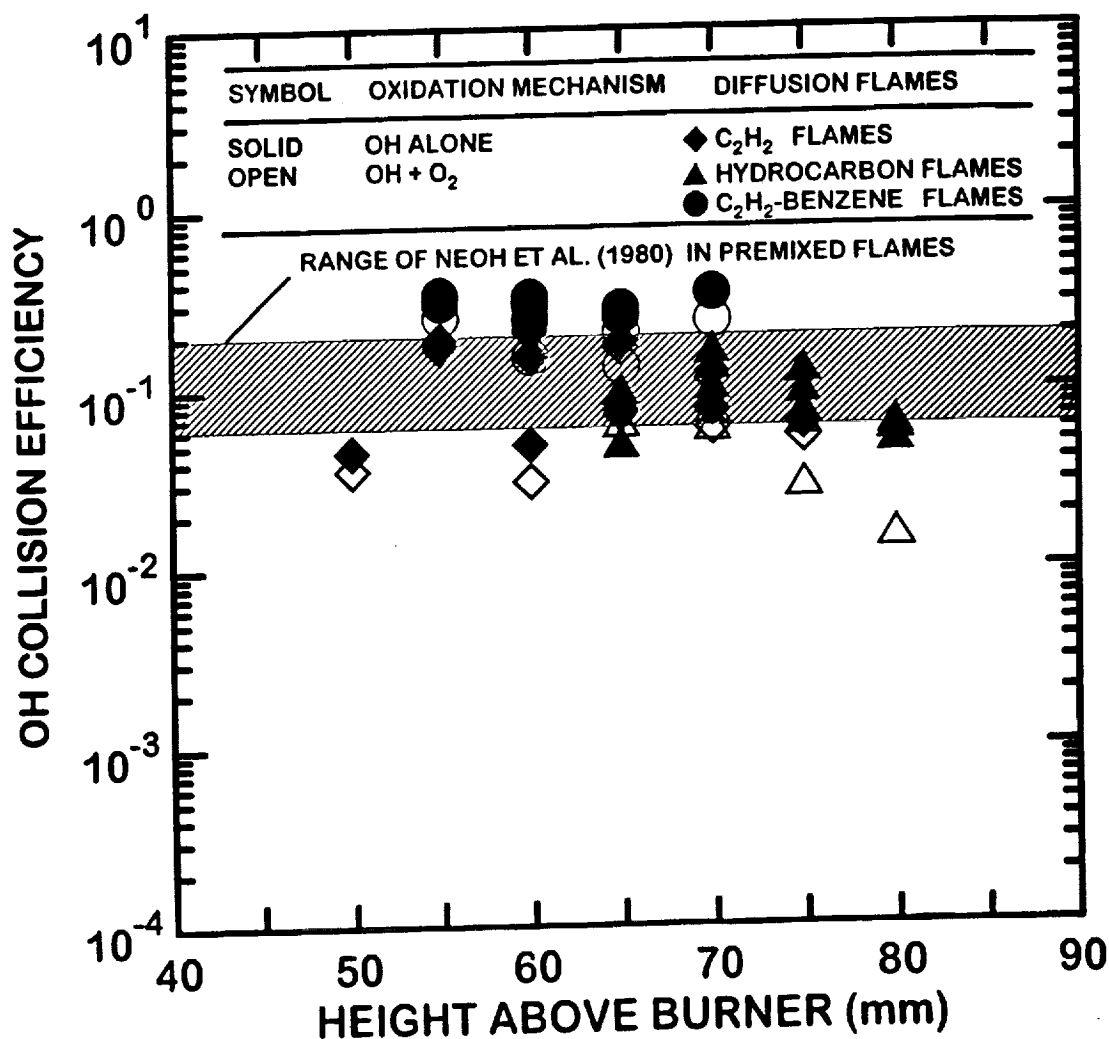
Fig. 12 Collision efficiencies assuming soot burnout due to attack by OH as a function of height above the burner at atmospheric pressure. Found from the measurements of Neoh et al. (1980) in premixed flames, and from present measurements in diffusion flames with and without parallel $O_2$ attack estimated from the predictions of Nagle and Strickland-Constable (1962). From Xu et al. (2001).

of soot estimated from the Nagle and Strickland-Constable (1962) results is not very important for these conditions, as before. On the other hand, similar to the observations of Neoh et al. (1980), present collision efficiencies of OH exhibit relatively small levels of scatter (roughly a factor of 3). Furthermore, the results for premixed and diffusion flames in Fig. 12 exhibit remarkably good agreement with each other. In particular, the collision efficiency of OH for soot oxidation in the present diffusion flames is 0.10 with a standard deviation of 0.07, which is in excellent agreement with the value for soot oxidation from Neoh et al. (1980) in nonpremixed flames of 0.13 when using the same treatment of soot structure. Finally, this agreement was achieved over a relatively broad range of flame conditions for the combined results in premixed and diffusion flames, as follows: temperatures of 1570-1870 K, oxygen molar concentrations (% by volume) of 0.001-1.2% and levels of soot mass consumption smaller than 70% at atmospheric pressure. Whereas these results are helpful, however, the properties of the final stage of oxidation, where internal oxidation of primary soot particles becomes a factor, effects of pressure on soot oxidation, and possibly effects of fuel type on soot oxidation for hydrocarbons other than those considered here, merit additional study in the future.

### 3.4 Soot Nucleation

**Soot Nucleation Rate Properties.** Soot nucleation is complex and involves processes similar to soot growth to form large molecular weight soot precursor species, processes of coagulation of large molecules to form soot nucleation sites, and processes of dehydrogenation of coagulated soot precursor species in order to reach carbon concentrations typical of primary soot particles, among others. A reasonable hypothesis for soot nucleation, however, is that it is dominated by the rate of formation of large molecular weight soot precursor species whose rates of formation should be similar to rates of soot surface growth. Past work finds that soot nucleation rates are proportional to acetylene concentrations which tends to support behavior along these lines (Sunderland et al., 1995; Sunderland and Faeth, 1996; Lin et al., 1996; Xu et al.,1997,1998). Based on these observations, a crude correlation of soot nucleation rates was attempted in terms of acetylene and H concentrations, and the temperature, as follows:

$$w_n = k_n(T)[C_2H_2][H] \tag{10}$$

where a correlation of $k_n(T)$ was sought in terms of an Arrhenius expression. The available database to test this expression include measurements of $w_n$ in premixed flames due to Xu et al.(1997,1998) and in diffusion flames due to Xu and Faeth (2001) and El-Leathy et al. (2001).

**Evaluation of the Soot Nucleation Rate Correlation.** Available measurements of soot nucleation rates are plotted in Fig. 13 as $k_n = w_n/([C_2H_2][H])$ as a function of reciprocal
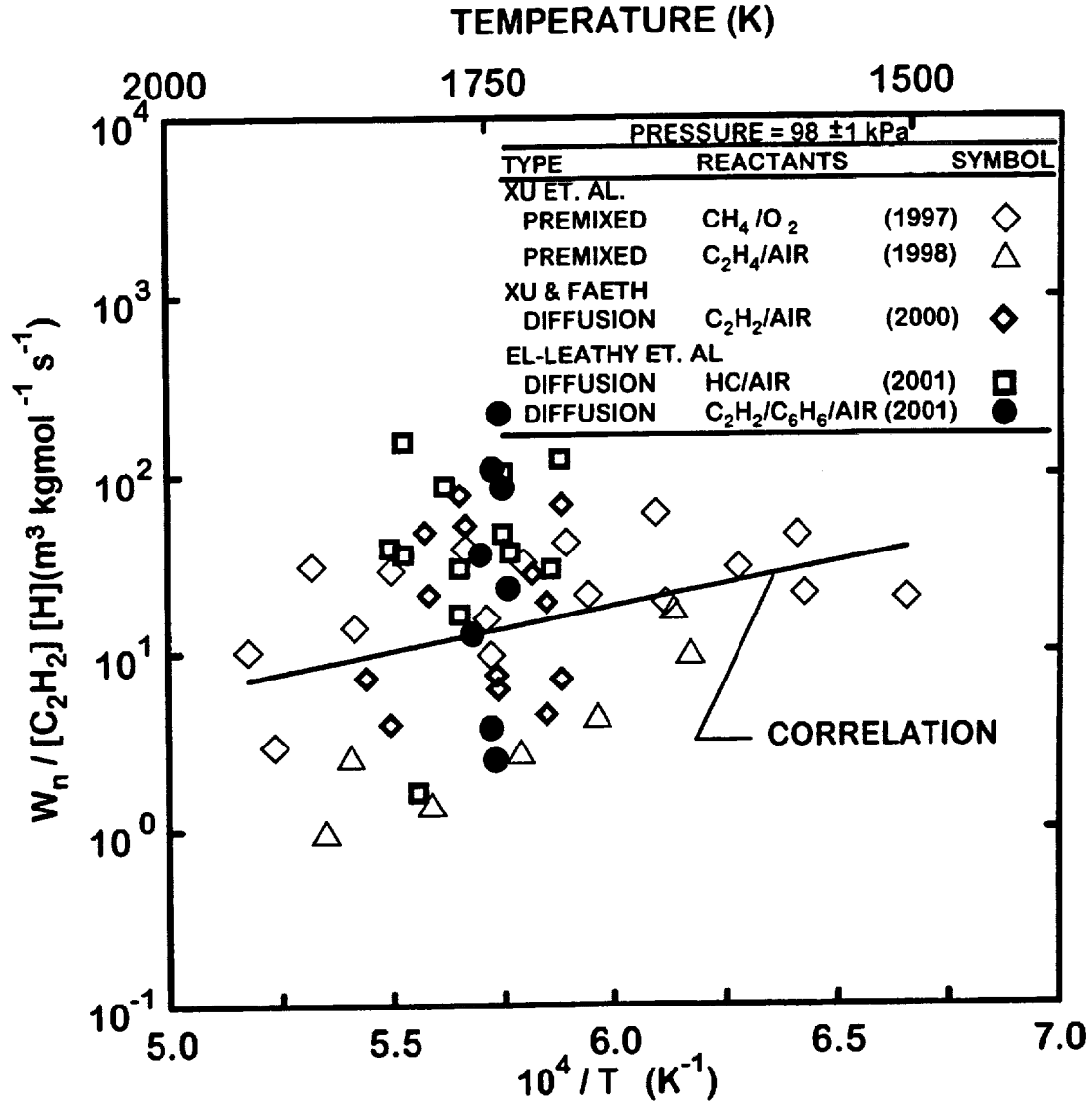
Fig. 13  Soot primary particle nucleation rates as a function of acetylene and hydrogen concentrations for laminar premixed and diffusion flames at atmospheric pressure. Measurements of ethylene/air premixed flames from Xu et al. (1997), measurements of methane/oxygen premixed flames from Xu et al. (1998), measurements of acetylene-nitrogen-air diffusion flames from Xu et al. (2001) and measurements of hydrocarbon-nitrogen/air diffusion flames of El Leathy et al. (2001).

temperature in order to assess an Arrhenius correlation of this function. Results for premixed and diffusion flames are reasonably consistent when plotted this way and yield a somewhat scattered correlation for $k_n(T)$ as follows (El-Leathy et al. (2001):

$$k_n = 0.018 \exp(11500/T) \qquad (11)$$

where $k_n$ ($m^3$/(kgmol-s)) and T(K). The range of data used to find Eq. (11)is as follows: acetylene mole fractions (% by volume) of 0.1-20%, H mole fractions of (by volume) of 0.03-3.0 ppm and temperatures of 1500-2100 K at atmospheric pressure, see El-Leathy et al. (2001) for a discussion of these findings.

Achieving some merging of primary particle nucleation rates in premixed and diffusion flames, as seen in Fig. 13, is encouraging, however, improved models of this process that achieve less scattered results and properly account for the detailed chemical and physical processes responsible for nucleation clearly are needed.

## 3.5 Conclusions

The soot reaction properties of soot surface growth, early soot surface oxidation (prior to oxidation mass consumptions of 70%) and soot nucleation were studied in the ethylene/air and methane/oxygen laminar premixed flames summarized in Table 3 and in the hydrocarbon air laminar jet diffusion flames summarized in Table 4, all of which were at atmospheric pressure. Major conclusions drawn from these observations are as follows:

1.    Soot surface growth rates in laminar premixed and diffusion flames are in reasonably good agreement with each other and could be correlated by the HACA soot growth mechanisms of Frenklach et al. (1990,1994), Kazakov et al. (1995) and Colket and Hall (1994). The steric factors found for these mechanisms had reasonable values on the order of unity and their values were similar for premixed and diffusion flame environments.

2.    Early soot oxidation rates were not correlated effectively with $O_2$, $CO_2$, $H_2O$ and O collision rates but could be correlated assuming a constant collision efficiency of 0.10 for OH in the present diffusion flames. This finding is in good agreement with the study of early soot oxidation in premixed flames due to Neoh et al. (1980). In contrast, direct soot oxidation by $O_2$, estimated from the results of Nagle and Strickland-Constable (1962), was negligible for the present flame environments.

3. Soot primary particle nucleation rates in laminar premixed and diffusion flames were similar for comparable temperatures and concentrations of H and acetylene. A crude correlation of soot primary particle nucleation rates was achieved using these variables but a more complete model of soot nucleation that accounts for soot precursor species and processes of coalescence, dehydrogenation, etc., should be sought in order to achieve a more complete and robust treatment of soot nucleation.

## 4. Laminar Diffusion Flame Studies (Ground- and Space-Based Studies)

### 4.1 Introduction

Laminar diffusion flames are of interest because they provide model flame systems that are far more tractable for analysis and experiments than more practical turbulent diffusion flames. Certainly, understanding flame processes within laminar diffusion flames must precede understanding these processes in more complex turbulent diffusion flames. In addition, many properties of laminar diffusion flames are directly relevant to turbulent diffusion flames using laminar flamelet concepts. Laminar jet diffusion flame shapes (luminous flame boundaries) have been of particular interest since the classical study of Burke and Schumann (1928) because they are a simple nonintrusive measurement that is convenient for evaluating flame structure predictions. Thus, consideration of laminar flame shapes is undertaken in the following, emphasizing conditions where effects of gravity are small, due to the importance of such conditions to practical applications.

Another class of interesting properties of laminar diffusion flames are their laminar soot and smoke point properties (i.e., the flame length, fuel flow rate, characteristic residence time, etc., at the onset of soot appearance in the flame (the soot point) and the onset of soot emissions from the flame (the smoke point)). These are useful observable soot properties of nonpremixed flames because they provide a convenient means to rate several aspects of flame sooting properties: the relative propensity of various fuels to produce soot in flames; the relative effects of fuel structure, fuel dilution, flame temperature and ambient pressure on the soot appearance and emission properties of flames; the relative levels of continuum radiation from soot in flames; and effects of the intrusion of gravity (or buoyant motion) on emissions of soot from flames. An important motivation to define conditions for soot emissions is that observations of laminar jet diffusion flames in critical environments, e.g., space shuttle and space station facilities, cannot involve soot emitting flames in order to ensure that test chamber windows used for experimental observations are not blocked by soot deposits, thereby compromising unusually valuable experimental results. Another important motivation to define conditions where soot is present in diffusion flames is that flame chemistry, transport and radiation properties are vastly simplified